Mechanics Research Communications

On the Severity of Aortic Stenosis in Ascending Aortic Aneurysm A Computational Tool to Examine Ventricular-Arterial Interaction and Aortic Wall Stress

--Manuscript Draft--

Manuscript Number:	
Article Type:	Full Length Article
Keywords:	ascending thoracic aortic aneurysm; aortic stenosis; shear stress; CFD; finite-element analysis
Corresponding Author:	Salvatore Pasta ITALY
First Author:	Federica Cosentino
Order of Authors:	Federica Cosentino
	Marzio Di Giuseppe
	Valentina Agnese
	Giovanni Gentile
	Giuseppe M Raffa
	Andrew Wisneski
	Julius Guccione
	Michele Pilato
	Salvatore Pasta
Abstract:	An ascending thoracic aortic aneurysm (ATAA) is a life-threatening cardiovascular consequence of vessel dilatation that portends adverse events and death. From a clinical perspective, ATAA should not be treated as an isolated disease, and surgery is often carried out in the presence of AS, aortic insufficiency or a calcified valve leaflet. Aortic stenosis (AS) is common in ATAAs and leads to both vessel rigidity and left ventricular (LV) impairment. In this study, lumped-parameter modeling and computational analysis were used to assess the change in the wall shear stress (WSS) and intramural wall stress of patient-specific ATAA models with different degrees of AS (ie, mild to severe). The ATAAs of four patients were reconstructed from imaging data and AS was simulated virtually using the lumped-based CircAdapt tool using clinical and echocardiographic data. Results show that LV work derived from pressure-volume loops increased with the severity of AS. Post-stenotic hemodynamic and structural variables markedly increased with AS severity, with WSS showing a 10-fold increase for the most severe AS model as compared to the baseline model with a well-functioning aortic valve. Most importantly, the increase in WSS and aortic wall stress was associated with pronounced values of valvulo-arterial impedance as an indicator of LV dysfunction. This study provides novel insights into progression of AS in patients with ATAAs at high risk of adverse events, and the potential value of valvulo-arterial impedance to predict changes in hemodynamic and structural parameters with the severity of AS.
Suggested Reviewers:	Christoph Sinning c.sinning@uke.de expert on cardiovascular domain
	marco Ciccone marcomatteo.ciccone@uniba.it clinical expert on cardiovascular domain
	massimo Capoccia capoccia@doctors.org.uk expert on the aortic stenosis

Opposed Reviewers:	

Title: Simulation of LVOT Obstruction in Transcatheter Mitral Valve-In-Ring Replacement

Authors: Federica Cosentino, Marzio Di Giuseppe, Valentina Agnese, Giovanni Gentile, Giuseppe M Raffa, Andrew Wisneski, Julius Guccione, Salvatore Pasta, Michele Pilato

Highlight:

- 1D modeling coupled with 3D computational flow analysis was used to assess the change in the hemodynamic and structural mechanics of ascending aortic aneurysm with virtual degree of aortic stenosis
- Post-stenotic wall and shear stresses exerted on the aneurysmal aortic wall increase non-linearly from the severity of aortic stenosis
- The increases in shear and principal stress with AS severity are associated with LV impairment as evaluated valvulo-arterial impedance.
- This study can provide novel insights into the progression of aortic stenosis in patients with stable aortic aneurysm dilatation at high risk of dissection and rupture during surveillance imaging

On the Severity of Aortic Stenosis in Ascending Aortic Aneurysm: A Computational Tool to Examine Ventricular-Arterial Interaction and Aortic Wall Stress

Federica COSENTINO[1], Marzio DI GIUSEPPE[1], Valentina AGNESE[2], Giovanni GENTILE[3], Giuseppe M RAFFA[2], Andrew WISNESKI[4], Julius GUCCIONE[4], Salvatore PASTA[5], Michele PILATO[2]

1 Department of Department of Health Promotion, Mother and Child Care, Internal Medicine and Medical Specialties, University of Palermo, Palermo, Italy
2 Department for the Treatment and Study of Cardiothoracic Diseases and Cardiothoracic Transplantation, IRCCS-ISMETT, Palermo, Italy
3 Department of Diagnostic and Therapeutic Services, Radiology Unit, IRCCS-ISMETT, Palermo, Italy
4 Department of Surgery, University of California San Francisco, San Francisco, Calif, USA
5 Department of Engineering, Viale delle Scienze, Ed.8, 90128, University of Palermo, Palermo, Italy

* Corresponding author:
Salvatore Pasta, PhD
Professor of Industrial Bioengineering,
Phone: +39 091 3815681
FAX: +39 091 3815682
e-mail: salvatore.pasta@unipa.it

Abstract

An ascending thoracic aortic aneurysm (ATAA) is a life-threatening cardiovascular consequence of vessel dilatation that portends adverse events and death. From a clinical perspective, ATAA should not be treated as an isolated disease, and surgery is often carried out in the presence of AS, aortic insufficiency or a calcified valve leaflet. Aortic stenosis (AS) is common in ATAAs and leads to both vessel rigidity and left ventricular (LV) impairment. In this study, lumped-parameter modeling and computational analysis were used to assess the change in the wall shear stress (WSS) and intramural wall stress of patient-specific ATAA models with different degrees of AS (ie, mild to severe). The ATAAs of four patients were reconstructed from imaging data and AS was simulated virtually using the lumped-based CircAdapt tool using clinical and echocardiographic data. Results show that LV work derived from pressure-volume loops increased with the severity of AS. Post-stenotic hemodynamic and structural variables markedly increased with AS severity, with WSS showing a 10-fold increase for the most severe AS model as compared to the baseline model with a well-functioning aortic valve. Most importantly, the increase in WSS and aortic wall stress was associated with pronounced values of valvulo-arterial impedance as an indicator of LV dysfunction. This study provides novel insights into progression of AS in patients with ATAAs at high risk of adverse events, and the potential value of valvulo-arterial impedance to predict changes in hemodynamic and structural parameters with the severity of AS.
Keywords: ascending thoracic aortic aneurysm; aortic stenosis; shear stress; CFD; finite-element analysis.

INTRODUCTION

An ascending thoracic aortic aneurysm (ATAA) is a cardiovascular condition that leads to permanent dilatation of the vessel and a high risk of adverse events when aortic size is >5cm [1]. Nearly 10 out of 100,000 persons per year are affected by ATAA [2], and in those with a bicuspid aortic valve (BAV), the prevalence of aortopathy ranges from 20-84% [3]. The risk of ATAA development in BAV patients was found to be 80-fold higher than for the general population with a morphologically-normal tricuspid aortic valve (TAV) [4]. Although the likelihood of rupture and dissection rises sharply for aneurysms that reach ≥6cm [1], the maximum aortic diameter is not necessarily a good predictor of rupture or dissection in patients with ATAAs [5].

Clinical recommendations for elective repair of ATAAs suggests surgery for an aortic diameter ≥5.5cm in the presence of a well-functioning aortic valve and the absence of risk factors or familiarities [6]. However, coexisting conditions of aortic stenosis (AS) or aortic insufficiency (AI) may heighten mortality associated with ATAA. Aortic dissection appears to be a rare event (~1%) in patients during a prolonged surveillance imaging and stable dilatation of the aneurysmal ascending aorta [7]. For certain patients, ATAA should not be treated as an isolated condition, and surgery to repair the aorta is often done in the presence of AS, AI or a calcified valve leaflet. Several clinical studies have demonstrated that repair of both the dilated aorta and its valve offer patients better longer term outcomes than isolated aortic valve replacement alone [7, 8].

Studies based on 4D cardiac MRI [9] and computational flow analyses [10-12] demonstrated that even a normally functioning BAV has altered flow and increased wall shear stress (WSS), thereby suggesting a hemodynamic origin of the bicuspid aorthopathy. Finite-element analysis also demonstrated increased wall stress in BAV ATAA versus TAV ATAA [13], increased risk of aortic dissection of BAV ATAA [14], stiffening of the aortic wall in ATAAs [15, 16], and the value of stress analysis to stratify the risk of rupture of the aneurysmal ascending aorta [17-19]. The presence of AS is associated with ascending aortic rigidity, where the degenerative process of stenosis involves impairment of left ventricular (LV) function.

This study offers preliminary data on the biomechanical association between aortic stenosis and ATAA biomechanics. This was accomplished by assessing the changes in the hemodynamic and structural forces exerted on the ATAA wall and LV function with the severity of AS. Using imaging data from four ATAA patients (two with BAV ATAA and two with TAV ATAA) and no valve dysfunction, virtual models of AS severity were developed using lumped-parameter modeling and computational analyses. The changes in wall shear stress (WSS) and principal stress were evaluated at under different degrees of AS and left-ventricular pressure-volume loops were quantified to determine ventricular-arterial interaction. The clinical implication of these findings are discussed.

MATERIAL AND METHODS

ATAA segmentation and meshing

Computed tomography angiography (CTA) scans of four patients with ATAA were identified from radiologic records of ISMETT IRCCS hospital as reported in similar studies [20, 21]. We selected two BAV ATAAs and two TAV ATAAs with aortic dilatation involving the ascending aorta (Type A) and the aortic root (Type N) [22]. BAV ATAAs were characterized by the right-left leaflet cusp fusion. For each patient, aortic valve function was assessed by Doppler echocardiography, with no signs of AS or AI. The study was approved by our ethics committee, and informed consent was obtained from the patient. From the CTA scan, the phase with the largest orifice area was reconstructed from the multiphase dataset. Semi-automatic thresholding and region growing techniques combined with manual editing of masks were used to determine the whole aorta and its valve (when fully-open) using Mimics software (Materialize NV, Leuven, Belgium). Segmented ATAA models were exported as STL mesh files to generate the element grid using ICEM software (Ansys v.18, ANSYS, Inc., Canonsburg, USA). For convergence of fluid-dynamic simulations, a mesh quality check was determined using grid convergence index analysis as assessed in a previous study of ATAA hemodynamics [23].

Lumped-parameter model

To assess cardiac mechanics and inlet boundary flow conditions of the stenotic aortic valve, the CircAdapt open-source cardiovascular tool (www.circadapt.org/) developed in the mathematical language program Matlab (The MathWorks, Inc, Natick, MA) was used to model the heart and circulation [24]. The CircAdapt is a zero-dimensional whole heart tool designed as a network composed by different modules including i) a deformable mayocardial wall with interventricular septum motion, ii) the cardiac valve hemodynamic and iii) the three-element Windkessel modeling of pulmonary and systemic circulations. The flow through the aortic valve is generated using the Bernoulli equation, assuming incompressibility and inviscid, irrotational flow. This approach allows for simulation of a phenomenological valve opening and closing function by changing the orifice area and then the pressure gradient across the aortic valve. CircAdapt was successfully used to simulate aortic valve insufficiency under different grades [25].

Starting from the reference simulation at rest condition, the CircAdapt cardiac and vascular parameters were calibrated using clinical and echocardiographic data to obtain a patient-specific simulation of the normal patient condition (Figure 1). The systemic arterial compliance was calculated as $SAC = SV_i/\Delta P$ where SV_i is the stroke volume indexed by body surface area and ΔP is pulse pressure as measured by echocardiography and cuff measurements, respectively.

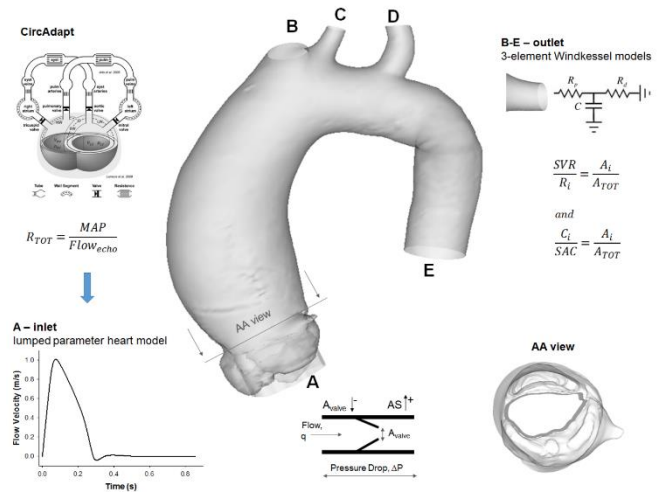

Figure 1: Problem specification of lumped-parameter model and computational flow analysis

Similarly, the systemic vascular resistance was SVR=80 x MAP/CO where MAP is the mean arterial pressure and CO is the cardiac output. Then, the SAC, SVR, patient heart rate and CO were set in the CircAdapt algorithm as reference parameters. The orifice area measured from CTA imaging was also set as input in CircAdapt. Thus, the arterial stiffness coefficient was iteratively adjusted to match the end-systolic and end-diastolic LV volumes. In this way, the peak flow velocity from the aortic valve derived from the lumped-parameter model corresponded well with transaortic flow velocity measured by Doppler echocardiography for each patient (error <5%). Once the normal condition was achieved for each patient, the severity of AS was simulated by virtually reducing the orifice area to obtain peak flow velocity of 2.5m/s (mild AS), 3.5m/s (moderate AS), and 4.5m/s (severe AS). The velocity profile was used as the input for the fluid-dynamic simulation (see Figure 2) whereas the pressure-volume loops were analyzed for each patient.

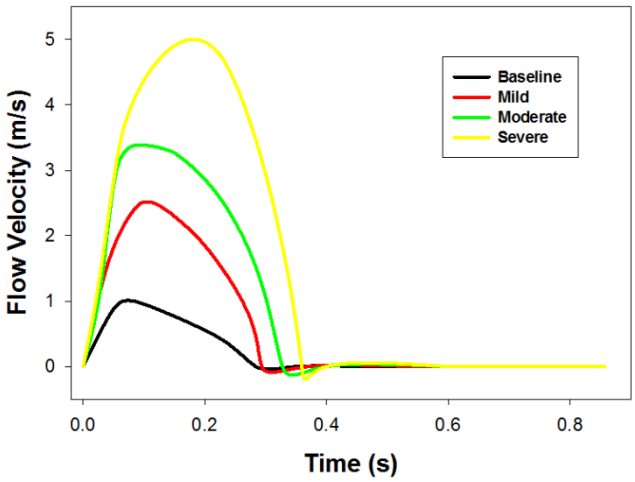

Figure 2: Pulsatile flow waveform used as boundary condition for Patient (D) to simulate the severity of AS

Fluid-dynamic analysis

Computational flow analyses were evaluated by unsteady simulations according to our previously developed approach using FLUENT solver (Ansys v.18, ANSYS, Inc., Canonsburg, USA) [10, 20, 26]. The blood was assumed to be an incompressible laminar-flow fluid with non-Newtonian viscosity described by the Carreau model and blood density of 1060kg/m^3. Pressure-implicit with splitting of operators and skewness correction as pressure–velocity coupling as pressure interpolation method with 2nd order accurate discretization were used. Convergence was enforced by reducing the residual of the continuity equation by 10−6 at every time step fixed to 0.005s. For boundary conditions, the pulsatile inlet flow waveform determined by the lumped-parameter model at normal and AS-related conditions was set at the inlet using profile data in FLUENT. The inlet was extended three-fold normal to the orifice area to ensure a fully-developed flow after the aortic valve. For outflow boundary conditions, SAC and SVR derived from clinical data were adopted to compute a three-element Windkessel model coupled to the supra-aortic vessels and the descending aorta (see Figure 1). Specifically, the proximal and total resistance of each individual branch was calculated using the relationship $SVR/R_i=A_i/A_{TOT}$ where A_i is the cross-sectional area of the individual outlet and A_{TOT} is the total cross-sectional area of all outlets in the ATAA model. We assumed the ratio of the proximal to the total resistance of 0.056 as suggested by Youssefi et al [11]. Similarly, the flow and compliance of each individual outlet was proportional to the outlet area: $C_i /SAC=A_i/A_{TOT}$. A set of resistance and compliance was obtained for each degree of AS. Simulations were continued through three cycles to eliminate nonlinear start-up effects, and results presented here were obtained at the last cardiac cycle.

Structural Analysis

To determine intramural stress at peak systole, pressure load forces at each node of the ATAA wall were exported from FLUENT and then imported in finite-element model developed in ABAQUS (SIMULIA Inc, Providence, USA). The anisotropic hyperelastic Holzapfel–Gasser–Ogden material model was used to characterize the mechanical behavior of the ATAA wall using mean values of material descriptors previously determined by our group [27]. Specifically, BAV ATAA had material descriptors (C_1=7.6kPa, k_1=110.2kPa, k_2=16.8, k=0.25) different from those of TAV ATAA (C_1=4.0kPa, k_1=113.8kPa, k_2=14.6, k=0.27). Local coordinate systems were defined for each ATAA model to include fiber orientation (θ=40deg for BAV ATAA and θ=34deg for TAV ATAA). Uniform material properties and thickness (1.8mm for BAV ATAA and 2.0mm for TAV ATAA) for the aortic wall were used. Distal ends of supra-aortic vessels, aortic valve and descending aorta were fixed in all directions, and the solution was obtained using Dynamic/Implicit formulation assuming a structural density of 1060kg/m^3.

Quantification of Hemodynamic and Structural Variables

As an index of LV work, valvulo-arterial impedance was evaluated for each patient scenario as the ratio of LV systolic pressure to SV_i. From each flow analysis, the maxima of peak systolic WSS and the time-averaged wall shear stress (TAWSS) over one cardiac cycle were evaluated. The helical flow index (HFI) as an index of complex, fully three dimensional flow fields according to Morbiducci et al. (this variable has a range of $0 \leq HFI \leq 1$ with 0 for irrotational flow) was quantified. From structural analyses, the intramural stress was quantified with the maximum principal stress of ATAA wall.

RESULTS

Figure 3 shows the pressure-volume loops predicted by the lumped-parameter model for each patient at different degrees of AS. A leftward shift of pressure-volume loops was observed as the AS increases from the baseline condition to the severe condition. The severity of AS augments total LV work, with blood pressure rising sharply during systole to a domed-shaped pressure-volume loop. SV tends to slightly reduce while valvulo-arterial impedance rises with stenosis severity.

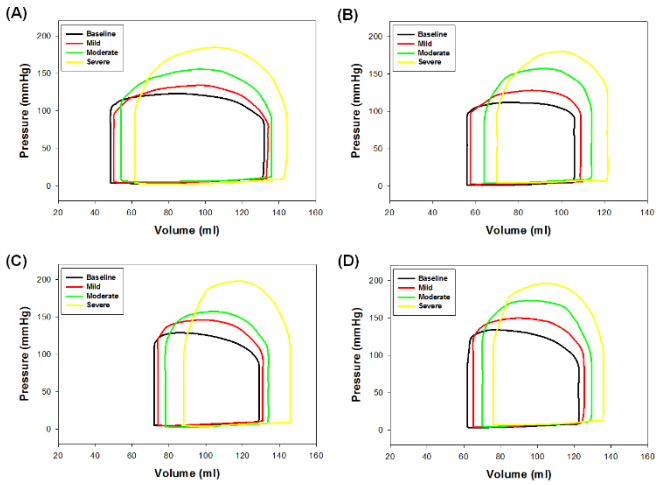

Figure 3: Pressure-volume loops at different degrees of AS for each patient: (A) BAV ATAA with Type A; (B) BAV ATAA with Type N; (C) TAV ATAA with Type A; (D) TAV ATAA with type N

Figure 4 displays a colored map of flow streamlines, TAWSS and principal stress at baseline condition for each patient. At peak systole, flow streamlines evinced a nested helical flow characterized by high peripheral flow velocity near the ATAA wall and slightly-helical moving flow in the aneurysm center. Movie 1 shows the flow field at different stage of the cardiac cycle for Patient (D) showing the largest aneurysm diameter among all patients. Maxima of TAWSS were found at mid-height of the ascending aorta for patients with tubular dilatation of the aorta (ie, Type A) and near the sino-tubular junction for patients with aortic root dilatation (ie, Type N). Conversely, peak values of maximum principal stress were found in the minor curvature of the ATAA wall for both BAV ATAA and TAV ATAA.

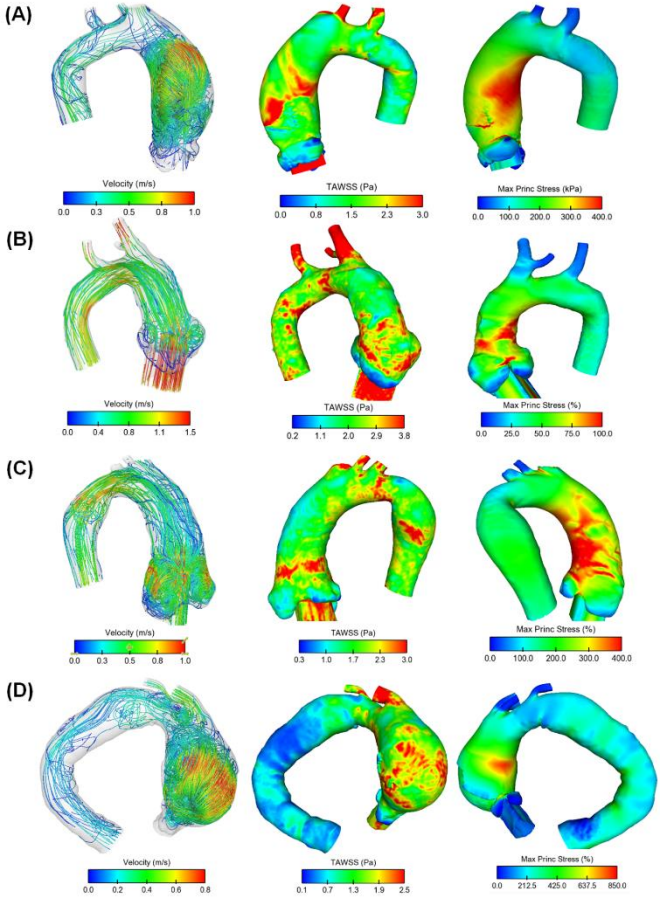

Figure 4: Flow streamlines (left column), maps of TAWSS (middle column) and maximum principal stress (right column) as determined at baseline configuration: (A) BAV ATAA with Type A; (B) BAV ATAA with Type N; (C) TAV ATAA with Type A; (D) TAV ATAA with type N

Figures 5 and 6 show the map of peak systolic WSS and maximum principal stress from baseline to the severe AS scenario for each patient. The peak values of hemodynamic and structural parameters were extrapolated at the same element node and then normalized by the baseline value. Figure 7 demonstrates that maximum principal stress and fluid shear have a non-linear steep increase from the mild to the severe stenotic model. Peak values of TAWSS for severe AS were 2.5 to 6-fold greater than the baseline values, whereas peak systolic WSS for severe AS was varied 10 times more than in the baseline model. Maximum principal stresses for the severe AS model were nearly twice those of the baseline model, except for Patient (D), which had a 4-fold increase in the minor curvature of the ascending aorta. The HFI was high for mild AS but decreased from moderate to severe AS because of the pronounced flow jet in the ascending aorta reducing the formation of helical flow.

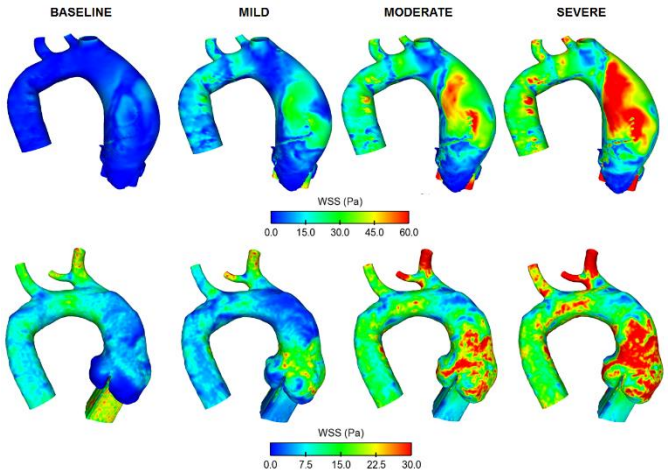

Figure 5: Peak systolic WSS for Patients (A) and (B)

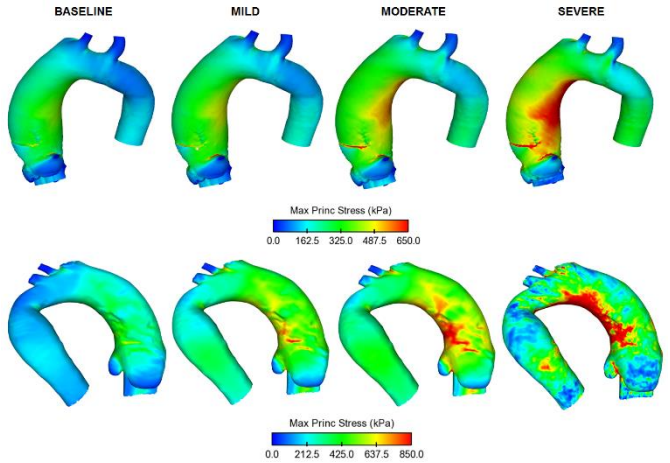

Figure 6: Principal stress map for Patients (A) and (C)

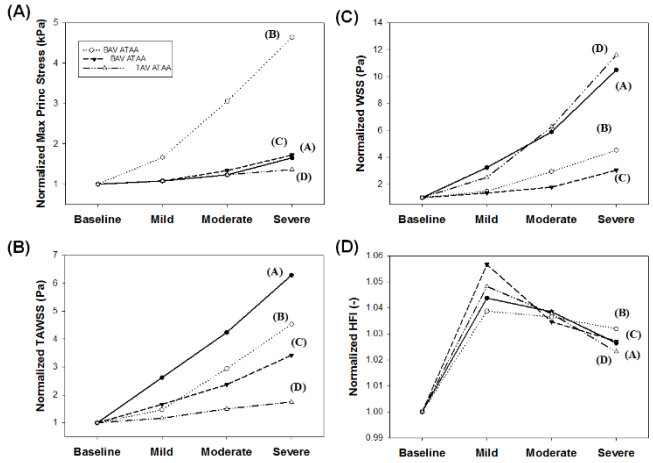

Figure 7: Profile of normalized (A) maximum principal stress, (B) WSS, (C) TAWSS and (D) HFI as function of AS severity: (A) BAV ATAA with Type A; (B) BAV ATAA with Type N; (C) TAV ATAA with Type A; (D) TAV ATAA with type N

Most interestingly, valvulo-arterial impedance and SV_i as indices of the LV load have a strong linear relationship with WSS and maximum principal stress as shown by Figure 8. The greater the aortic wall and shear stresses, the greater is the valvulo-arterial impedance and thus the greater the LV stroke for ejecting the blood volume. In all cases, the goodness-of-fit measure was R^2>0.95 for both the WSS and principal stress parameters.

Figure 8: Linear regression of maximum principal stress

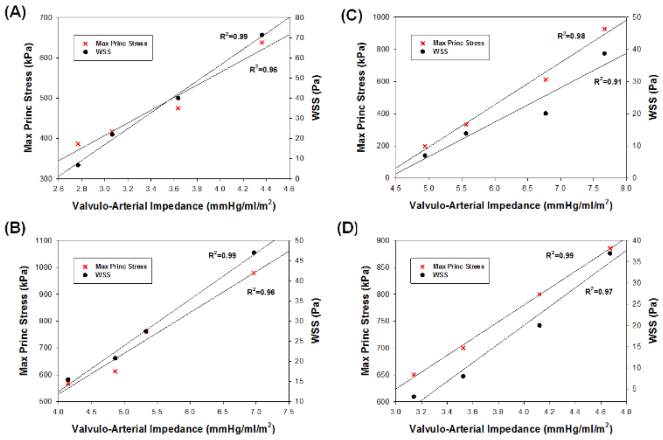

and WSS with valvulo-arterial impedance for all patients: (A) BAV ATAA with Type A; (B) BAV ATAA with Type N; (C) TAV ATAA with Type A; (D) TAV ATAA with type N

DISCUSSION

We adopted a computational framework to assess the change in the hemodynamic and structural mechanics of ATAAs under different degrees of AS. The ventricular-arterial interaction modeling approach demonstrated that post-stenotic wall and shear stresses exerted on the ATAA increase non-linearly from the baseline configuration of a patient with no signs of valvulopathy to the virtual model with severe AS. Specifically, peak systolic WSS for the model with severe AS rose up to 10-fold with respect to the baseline model whereas the maximum principal stress difference between the baseline and the severe AS models rose up to 2-fold. Most importantly, the increases in WSS and principal stress with AS severity are associated with LV impairment as evaluated by SV_i and valvulo-arterial impedance. In this hypothesis-generating study, the altered post-stenotic blood flow in the setting of a dilated aorta is a potential cause of LV afterload and may serve as an indicator of adverse outcome in patients with ATAAs.

The coupling of a lumped parameter heart model with computational flow analysis represents a promising tool to reveal insights in the aortopathy progression. Kim et al [28] coupled a lumped-parameter heart model (to derive the pressure-volume loop) with a computational flow analysis of the aorta with coarctation at resting and exercise conditions. For the abdominal aorta, the coupling of a one-dimensional lumped parameter model to three-dimensional finite-element models evinced realistic representations of flow and pressure in the downstream branches and demonstrated the importance of using appropriate boundary conditions [29]. Indeed, outflow boundary condition based on three-element Windkessel has become the standard approach in computational flow analysis [11].

This study was motivated by clinical evidence on the progression of the aneurysmal ascending aorta commonly seen in patients with chronic ATAAs. In a long-term longitudinal study of 206 patients with ATAA, we recently discovered that the aneurysmal aorta dilates primarily in the first 2 years after diagnosis and then reaches a plateau to substantially remain stable over an 8-year follow-up period [30]. At in-hospital admission, aortic size of BAV ATAA versus TAV ATAA was comparable but bicuspid patients were younger than tricuspid patients and free of cardiovascular risk factors. Most importantly, patients with ATAA who developed severe AS or regurgitation during the long-term surveillance imaging period had the highest chances of being referred for surgical repair of the ATAA. These clinical observations are in agreement with other reports suggesting that isolated repair of the dilated ascending aorta is a less frequent surgical practice than the repair of both the aorta and its valve [6, 31]. Therefore, aortopathy should not be considered as an isolated disease but rather a concurrent vascular and valvular pathological condition. One argument supporting the repair of both the ATAA and aortic valve is the fact that aortic size is not a good predictor of adverse events even though the aortic wall tends to be quite thin when the diameter exceeds 4.5 cm [5]. Moreover, the presence of AS is a more common indication for ATAA surgery than the presence of AI [6].

The open question is therefore to understand how AS develops in a patient with stable aortic dilatation and the detrimental effect of valvular-related hemodynamic and structural loads on the onset of rupture and dissection. Though the mechanism underlying AS development cannot be easily assessed by computational tools, our study demonstrated abnormal alteration of WSS and principal stress with the severity of AS. The latter poses additional afterload on the LV function so that the index of valvulo-arterial impedance (ie, the cost in mmHg for each millimeter of blood pumped by the LV at systole) can be used to quantify the double vascular and valvular load occurring in stenotic ATAAs. According to our analysis, the LV work is directly related by robust linear relationships (R^2>0.95 in all patient cases) to the post-stenotic alterations of peak systolic WSS and principal stress on the ATAA wall, and this highlights the future usefulness of this index to determine the risk of complications with the progression of ATAA development. Thus, using a clinically measurable parameter of cardiac function, we can predict the increase in WSS and wall stress without the need for simulating ATAA mechanics.

Bicuspid patients with AS and ATAA had an increased risk of aortic rupture, dissection, or death before operative repair when compared with patients with a normally functioning bicuspid valve [2]. However, computational studies [15] and ex-vivo biomechanical testing [32] demonstrated that physiological stress in ATAAs is far away from rupture and that only a hypertensive scenario can engender stress sufficient enough to cause rupture . A computational flow study demonstrated that a stiff ATAA may have the most altered distribution of wall stress and that an acute change of peripheral vascular resistance could significantly increase rupture risk [15]. Here, we similarly speculate that AS can lead to high hemodynamic and structural loads to cause complications of the dilated ascending aorta. Although we cannot to assess at which degree of AS the adverse event manifests, finite-element analysis is considered to be the most versatile tool to assess the likelihood of rupture by wall stress comparison between ruptured and unruptured ATAAs [18].

There are a number of limitations in this work. The CircAdapt tool was not fully coupled to the computational flow analysis. However, even in a strongly-coupled approach between lumped-parameter and finite-element simulations, the ventricular pressure and volume are independent of the computational flow model because the interaction occurs only during cardiac ejection [28]. We did not consider wall compliance in our computational flow study. However our experience in ATAA modeling suggests no differences between rigid and compliant vessel mechanics as the systolic-to-diastolic aortic diameter change in ATAAs is very low (ie, aortic diameter of 41.4±5.2mm at systole and 39.9±5.4mm at diastole, n=206 patients) [33].

CONCLUSION

In this study, simulations were performed to assess the impact of post-stenotic shear and wall stresses in patients with ATAAs. As the stenosis increased from the baseline model with no signs of valvular dysfunction to the virtual model with severe AS, the WSS and maximum principal stress shown a 2.5- and 6-fold increase on the forces exerted on the ATAA wall, respectively. Hemodynamic and structural changes were associated with predictions of the valvular-arterial impedance, suggesting LV impairment and the potential to predict shear and wall stress changes with a clinical cardiac parameter. This framework can provide novel insights into the progression of AS in patients with stable ATAA dilatation at high risk of dissection and rupture during surveillance imaging.

ACKNOWLEDGMENT

This work was supported by a “Ricerca Finalizzata” grant from the Italian Ministry of Health (GR-2011-02348129) to Salvatore Pasta.

REFERENCES

[1] Elefteriades JA, Farkas EA. Thoracic aortic aneurysm clinically pertinent controversies and uncertainties. J Am Coll Cardiol. 2010;55:841-57.

[2] Davies RR, Kaple RK, Mandapati D, Gallo A, Botta DM, Jr., Elefteriades JA, et al. Natural history of ascending aortic aneurysms in the setting of an unreplaced bicuspid aortic valve. Ann Thorac Surg. 2007;83:1338-44.

[3] Verma S, Siu SC. Aortic dilatation in patients with bicuspid aortic valve. N Engl J Med. 2014;370:1920-9.

[4] Michelena HI, Prakash SK, Della Corte A, Bissell MM, Anavekar N, Mathieu P, et al. Bicuspid aortic valve: identifying knowledge gaps and rising to the challenge from the International Bicuspid Aortic Valve Consortium (BAVCon). Circulation. 2014;129:2691-704.

[5] Pape LA, Tsai TT, Isselbacher EM, Oh JK, O'Gara PT, Evangelista A, et al. Aortic diameter >= 5.5 cm is not a good predictor of type A aortic dissection - Observations from the international registry of acute aortic dissection (IRAD). Circulation. 2007;116:1120-7.

[6] Borger MA, Fedak PWM, Stephens EH, Gleason TG, Girdauskas E, Ikonomidis JS, et al. The American Association for Thoracic Surgery consensus guidelines on bicuspid aortic valve-related aortopathy: Full online-only version. J Thorac Cardiovasc Surg. 2018;156:e41-e74.

[7] Michelena HI, Khanna AD, Mahoney D, Margaryan E, Topilsky Y, Suri RM, et al. Incidence of aortic complications in patients with bicuspid aortic valves. JAMA. 2011;306:1104-12.

[8] Raffa G, Bryan W, Pasta S, Morsolini M, Pietrosi A, Scardulla C, et al. Patients with bicuspid aortic valve are likely to receive an aortic valve prosthesis during prophylactic resection of their ascending aortic aneurysm. International Journal of Cardiology. 2016;206:97-100.

[9] Mahadevia R, Barker AJ, Schnell S, Entezari P, Kansal P, Fedak PWM, et al. Bicuspid Aortic Cusp Fusion Morphology Alters Aortic Three-Dimensional Outflow Patterns, Wall Shear Stress, and Expression of Aortopathy. Circulation. 2014;129:673-82.

[10] Pasta S, Gentile G, Raffa GM, Bellavia D, Chiarello G, Liotta R, et al. In Silico Shear and Intramural Stresses are Linked to Aortic Valve Morphology in Dilated Ascending Aorta. European Journal of Vascular and Endovascular Surgery. 2017;S1078-5884(17)30331-3.

[11] Youssefi P, Gomez A, He T, Anderson L, Bunce N, Sharma R, et al. Patient-specific computational fluid dynamics-assessment of aortic hemodynamics in a spectrum of aortic valve pathologies. J Thorac Cardiovasc Surg. 2017;153:8-20 e3.

[12] Malvindi PG, Pasta S, Raffa GM, Livesey S. Computational fluid dynamics of the ascending aorta before the onset of type A aortic dissection. European Journal of Cardio-Thoracic Surgery 2016;doi: 10.1093/ejcts/ezw306

[13] Nathan DP, Xu C, Plappert T, Desjardins B, Gorman JH, 3rd, Bavaria JE, et al. Increased ascending aortic wall stress in patients with bicuspid aortic valves. Ann Thorac Surg. 2011;92:1384-9.

[14] Emerel L, Thunes J, Kickliter T, Billaud M, Phillippi JA, Vorp DA, et al. Predissection-derived geometric and distensibility indices reveal increased peak longitudinal stress and stiffness in patients sustaining acute type A aortic dissection: Implications for predicting dissection. J Thorac Cardiovasc Surg. 2018.

[15] Campobasso R, Condemi F, Viallon M, Croisille P, Campisi S, Avril S. Evaluation of Peak Wall Stress in an Ascending Thoracic Aortic Aneurysm Using FSI Simulations: Effects of Aortic Stiffness and Peripheral Resistance. Cardiovascular Engineering and Technology. 2018;9:707-22.

[16] Pasta S, Agnese V, Di Giuseppe M, Gentile G, Raffa GM, Bellavia D, et al. In-vivo Strain Analysis of Dilated Ascending Thoracic Aorta by ECG-gated CT Angiographic Imaging. Annals of Biomedical Engineering. 2017;45:2911-20.

[17] Gomez A, Wang Z, Xuan Y, Wisneski AD, Hope MD, Saloner DA, et al. Wall Stress Distribution in Bicuspid Aortic Valve-Associated Ascending Thoracic Aortic Aneurysms. Ann Thorac Surg. 2020.

[18] Wang Z, Flores N, Lum M, Wisneski AD, Xuan Y, Inman J, et al. Wall stress analyses in patients with >/=5 cm versus <5 cm ascending thoracic aortic aneurysm. J Thorac Cardiovasc Surg. 2020.

[19] Pasta S, Agnese V, Gallo A, Cosentino F, Di Giuseppe M, Gentile G, et al. Shear Stress and Aortic Strain Associations with Biomarkers of Ascending Thoracic Aortic Aneurysm. Ann Thorac Surg. 2020.

[20] Rinaudo A, D'Ancona G, Lee JJ, Pilato G, Amaducci A, Baglini R, et al. Predicting Outcome of Acute Aortic Dissection with Patent False Lumne by Computational Flow Analysis Cardiovascular Engineering and Technology. 2014;5:176-88.

[21] Pasta S, Gentile G, Raffa GM, Scardulla F, Bellavia D, Luca A, et al. Three-dimensional parametric modeling of bicuspid aortopathy and comparison with computational flow predictions. Artif Organs. 2017.

[22] Schaefer BM, Lewin MB, Stout KK, Gill E, Prueitt A, Byers PH, et al. The bicuspid aortic valve: an integrated phenotypic classification of leaflet morphology and aortic root shape. Heart. 2008;94:1634-8.

[23] Rinaudo A, Pasta S. Regional variation of wall shear stress in ascending thoracic aortic aneurysms. Proceedings of the Institution of Mechanical Engineers Part H, Journal of engineering in medicine. 2014;228:627-38.

[24] Lumens J. Creating your own virtual patient with CircAdapt Simulator. Eur Heart J. 2014;35:335-7.

[25] Palau-Caballero G, Walmsley J, Gorcsan J, 3rd, Lumens J, Delhaas T. Abnormal Ventricular and Aortic Wall Properties Can Cause Inconsistencies in Grading Aortic Regurgitation Severity: A Computer Simulation Study. Journal of the American Society of Echocardiography : official publication of the American Society of Echocardiography. 2016;29:1122-30 e4.

[26] Gallo A, Agnese V, Coronnello C, Raffa GM, Bellavia D, Conaldi PG, et al. On the prospect of serum exosomal miRNA profiling and protein biomarkers for the diagnosis of ascending aortic dilatation in patients with bicuspid and tricuspid aortic valve. Int J Cardiol. 2018;273:230-6.

[27] Pasta S, Phillippi JA, Tsamis A, D'Amore A, Raffa GM, Pilato M, et al. Constitutive modeling of ascending thoracic aortic aneurysms using microstructural parameters. Med Eng Phys. 2016;38:121-30.

[28] Kim HJ, Vignon-Clementel IE, Figueroa CA, LaDisa JF, Jansen KE, Feinstein JA, et al. On Coupling a Lumped Parameter Heart Model and a Three-Dimensional Finite Element Aorta Model. Annals of Biomedical Engineering. 2009;37:2153-69.

[29] Vignon-Clementel IE, Figueroa CA, Jansen KE, Taylor CA. Outflow boundary conditions for 3D simulations of non-periodic blood flow and pressure fields in deformable arteries. Comput Methods Biomech Biomed Engin. 2010;13:625-40.

[30] Agnese V, Pasta S, Michelena HI, Mina C, Romano GM, Carerj S, et al. Patterns of ascending aortic dilatation and predictors of surgical replacement of the aorta: A comparison of bicuspid and tricuspid aortic valve patients over eight years of follow-up. Journal of molecular and cellular cardiology. 2019;135:31-9.

[31] Raffa GM, Wu B, Pasta S, Morsolini M, Bellavia D, Romano G, et al. Patients with bicuspid aortic valve are likely to receive an aortic valve prosthesis during prophylactic resection of their ascending aortic aneurysm. Int J Cardiol. 2016;206:97-100.

[32] Duprey A, Trabelsi O, Vola M, Favre JP, Avril S. Biaxial rupture properties of ascending thoracic aortic aneurysms. Acta Biomater. 2016;42:273-85.

[33] Mendez V, Di Giuseppe M, Pasta S. Comparison of hemodynamic and structural indices of ascending thoracic aortic aneurysm as predicted by 2-way FSI, CFD rigid wall simulation and patient-specific displacement-based FEA. Computers in Biology and Medicine. 2018;100:221-9.

Video

Click here to access/download
Video
Movi_Velocity.avi